2010

Elastic conducting carbon nanotube-laden SIBS fibers

Alberto J. Granero
University of Wollongong

Joselito M. Razal
University of Wollongong, jrazal@uow.edu.au

Gordon G. Wallace
University of Wollongong, gwallace@uow.edu.au

Marc in het Panhuis
University of Wollongong, panhuis@uow.edu.au

Elastic conducting carbon nanotube-laden SIBS fibers

Abstract

We report a facile method to produce elastic conducting fibers using a continuous flow wet-spinning approach. The spun fibers were highly stretchable, similar to the elastomeric polymer used.

Publication Details

Granero, A. J., Razal, J. M., Wallace, G. G. & in het Panhuis, M. (2010). Elastic conducting carbon nanotube-laden SIBS fibers. (ICONN), 2010 International Conference on Nanoscience and Nanotechnology (pp. 80-83).

Elastic conducting carbon nanotube-laden SIBS fibers

Alberto J. Granero, Joselito M. Razal, Gordon G. Wallace, and Marc in het Panhuis
[1]ARC Centre of Excellence for Electromaterials Science, Intelligent Polymer Research Institute,
School of Chemistry, University of Wollongong,
Northfield Avenue, Wollongong, NSW 2522; Australia

***Abstract*—We report a facile method to produce elastic conducting fibers using a continuous flow wet-spinning approach. The spun fibers were highly stretchable, similar to the elastomeric polymer used.**

Keywords–fiber spinning, wet-spinning, carbon nanotube, conducting fibers, elastic fibers.

I. INTRODUCTION

Prior to 2002, when Boston Scientific Corporation introduced the TAXUS® coronary stent, poly(styrene-block-isobutylene-block-styrene) ("SIBS") was relatively unknown in medicine [1]. Medical SIBS is a biostable and biocompatible elastomer [2] which was developed as an alternative to polyurethanes as polyether, polyester and polycarbonate urethanes all undergo biodegradation *in vivo*. The mechanical properties of SIBS overlap silicone rubber and polyurethane and it has been successfully used as a drug eluting coating in coronary stents (TAXUS®). Furthermore, the viability of SIBS as an ophthalmic implant is being investigated for the treatment of glaucoma [3] as well as prosthetic material for synthetic trileaflet aortic valve replacement [4].

The creation of new composites based on elastomers combined with conducting materials has attracted the attention of scientists in the last decades. There is a growing number of publications related to composites consisting of elastomeric polymers and metallic particles [5], carbon black [6], conducting polymers [7] as well as carbon nanotubes (CNT) [8].

In addition to carbon nanotubes' electrical properties, their mechanical properties (stronger and lighter than steel) make CNT interesting fillers for elastomeric polymers. However, processing is an important issue as CNT are difficult to disperse in polymers because they tend to agglomerate [8]. In recent years carbon nanotubes have been used to provide electrical conductivity to SIBS [9, 10]. For example, Gilmore *et al.* [9] reported conductivities up to 10 S/cm and these composites supported the growth of L-929 cells. These results opened the door to biocompatible composites suitable for electrical stimulation of cells and tissue.

Fibers are versatile structures with promising applications in medical implants and devices. Recent studies have shown that fibers can direct the growth and migration of cells *in vitro* [11]. Fibers made of elastomeric polymers, such as SIBS, have been traditionally produced by melt-spinning process. However, this process is not suitable to produce SIBS/CNT composite fibers due to the laborious process of dispersing CNTs in a viscous medium such as a melt polymer. Carbon nanotubes can be dispersed in a solvent prior to mixing with SIBS, which is more conductive to the wet-spinning method. In this paper we demonstrate a simple continuous flow wet-spinning method to produce conducting SIBS/CNT composites.

II. EXPERIMENTAL

A. Materials

Medical grade SIBS, M_W 80,000 – 130,000 g/mol, batch no. 5000587522 was a gift from Boston Scientific Corporation. Octadecyl amine functionalized single walled carbon nanotubes (ODA-SWNT) were obtained from Carbon Solutions Inc. (P5-SWNT, Lot 05 139, 60 – 70% SWNT loading, 2 – 4% metal content). Toluene, tetrahydrofuran (THF) and methanol (all analytical reagent grade) were obtained from Univar and 1,2-dichlorobenzene (oDCB), 99%, was obtained from Sigma-Aldrich. All materials were used as received.

B. Fibre spinning

1) Wet-spinning

The wet-spinning process consists in the formation of a solid fiber from a solution (or dispersion) when this is introduced in a coagulation. Typically a polymer was dissolved in the appropriate solvent precipitated when injected in a medium where it was not soluble. The spinning dispersion was injected into the coagulation bath (methanol) using a 5 mL glass syringe and a syringe pump (KD Scientific, KDS100); the needle used had an inner diameter of 0.32 mm (23 gauge), (Fig. 1).

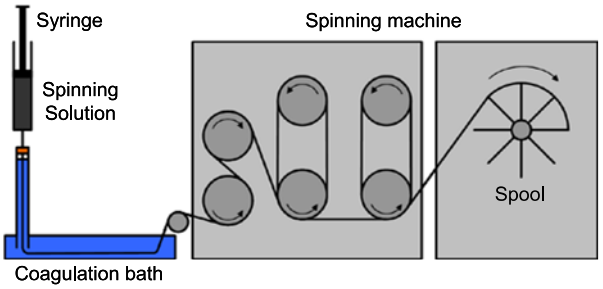

Figure 1. Schematic representation of the wet-spinning process.

The injected dispersion coagulated in the vertical stage. The fiber's own weight pulled it to the bottom end of that stage where it connected to the horizontal bath. The spinning machine pulled the fiber through the bath and out at the other end. This setup (Fig. 1) was able to produce fibers up to several meters in length, only limited by the volume of the injecting device.

2) *Choosing solvent/non-solvent system*

In order to find suitable solvents and coagulation baths Hildebrand solubility parameter can be used. SIBS had an estimated Hildebrand parameter of 16.5 $MPa^{½}$; calculated based on the styrene:isobutylene ratio (30:70) and their solubility values (17.8 $MPa^{½}$ [12] and 16.0 $MPa^{½}$ [12], respectively). SIBS should be soluble in liquids with similar Hildebrand parameters such as toluene (18.3 $MPa^{½}$ [13]), THF (19.5 $MPa^{½}$ [13]) or oDCB (20.5 $MPa^{½}$ [13]) and not soluble in those liquids whose Hildebrand solubility parameters are different from that of SIBS's, the larger the difference, the less soluble SIBS will be. For example, SIBS has limited solubility in 2-propanol (23.5 $MPa^{½}$ [12]) or methanol (29.7 $MPa^{½}$ [13]).

Three different batches of fibers were made to assess the most suitable solvent. SIBS (20% w/v) was dissolved in toluene, THF and oDCB, then fibers were made by coagulation in methanol. The mechanical properties of the fibers were studied by dynamic mechanical analysis (see the characterization section for more details).

3) *Spinning dispersions*

Spinning dispersions were prepared by dispersing first the ODA-SWNT in oDCB (Sonics VibraCell horn tip sonicator) for 20 min at 30% amplitude, in pulsed mode (2 s on / 1 s off). Dispersions were prepared with ODA-SWNT concentration of 0.4, 0.8, 1.2 and 1.8% w/v. Once the dispersions were deemed suitable for spinning (no visible aggregates at optical microscope) SIBS was dissolved in the dispersion to a polymer concentration of 10% w/v.

C. *Characterisation*

1) *Mechanical Testing*

Dynamic mechanical analysis was performed on the fibers using the model EZ-S from Shimadzu with a 2 N load cell. Samples were mounted on paper frames (10 mm in aperture) which were placed in 1 N sample holders (EZ-S clamps). The paper frame was cut after mounting the sample and this was strained at a crosshead speed of 10 mm/min (100 %/min) until breakage. The fiber's dimensions were determined using an optical microscope (Leica DM EP).

2) *Conductivity*

The fiber's resistance (R) was determined using an in-house 4-point probe design consisting of four electrodes aligned in parallel fashion, each 2 mm apart. Fibers were attached perpendicular to the electrodes using conducting silver paint to ensure electrical contact. A constant direct current (1 nA) was applied between the outer electrodes (eDAQ eCorder 401 coupled with a galvanostat) and voltage was recorded among the inner electrodes using a multimeter (Agilent 34410A). Conductivity (•) was calculated using the following equation:

$$\sigma = \frac{l}{R \cdot A}, \tag{1}$$

where l was the distance between the electrodes and A the cross sectional area of the fiber (determined by optical microscopy, Leica DM EP).

3) *Strain Gauging*

The evolution of the electrical properties of the fibers during periods of strain-relaxation was studied using an in-house experimental design. Samples were prepared for mechanical testing as described above. The paper frames were adapted to include two electrodes consisting of copper tape, (Fig. 2), to contact the sample. A constant potential (10 V) was using a power source (Powertech DC Power Supply, model MP-3087) and the current was monitored as a function of time using a digital multimeter (Agilent 34410A) hooked to a computer.

Samples were strained at 10 mm/min until reaching 30% strain. Then they were cyclically relaxed to 10% and strained back to 30% while the electrical properties were recorded. Conductivity was calculated, assuming the volume of the sample remained constant, using the following equation:

$$\sigma = \frac{l^2}{R \cdot l_0 \cdot A_0}, \tag{2}$$

where l_0 was the initial distance between the electrodes, l the distance between the electrodes at any given time and A_0 the cross sectional area of the fiber without any strain.

III. Results and Discussion

A. *Choosing solvent/non-solvent system*

The results, summarized in Table I, showed that fibers produced from THF solution were stiffer (higher Young's modulus values) and more brittle (lower strain before breakage values) than those made from toluene or oDCB.

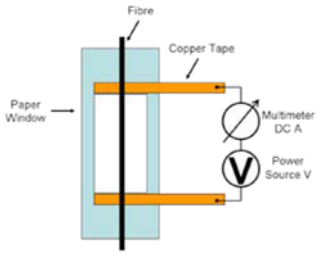

Figure 2. Schematic representation of the experimental design for simultaneous monitoring of stress-strain and electrical data.

TABLE I. DYNAMIC MECHANICAL ANALYSIS RESULTS ON FIBRES MADE OF 20 % W/V SIBS IN TOLUENE, THF AND ODCB; METHANOL USED AS COAGULATION BATH.

Solvent	Young's Modulus (MPa)	Tensile Strength (MPa)	Strain (%)
Toluene	3.2 ± 0.5	23.4 ± 2.4	1106 ± 133
THF	10.0 ± 1.0	3.0 ± 0.3	358 ± 36
oDCB	3.8 ± 0.9	15.0 ± 0.7	1071 ± 99

The fibers made from toluene or oDCB showed similar Young's modulus and ductility values. Despite fibers made from toluene showed higher tensile strength values, oDCB was chosen as solvent because it had been reported as a better medium to produce good quality CNT dispersions [14]. ODA-SWNT were chosen because their Hildebrand solubility parameter (19.5 $MPa^{½}$ [15]) was very close to oDCB's value.

B. *Mechanical testing*

The stiffness (Young's modulus) of samples increased with the addition of ODA-SWNT from 3.8 (0% w/v ODA-SWNT) to 5.7 MPa (1.8% ODA-SWNT). The tensile strength and ductility (maximum strain before breakage) values of fibers containing ODA-SWNT (6 – 7 MPa and 700 – 800% respectively) were lower than those from fibers spun without CNT (15 MPa tensile strength and 1070% strain), (Fig. 3). Stress focuses on the interface polymer/CNT leading to breakage of the fiber under lower loads. However, it is remarkable that tensile strength and ductility values remained independent of the ODA-SWNT concentration. This suggests the ODA-SWNT were not dispersed uniformly but they aggregated into clusters.

C. *Conductivity*

The electrical conductivity results of the spun fibers (Fig. 4) showed that the highest conductivity was 84 mS/cm, observed for a fiber prepared using a dispersion of 0.4% w/v ODA-SWNT and 10% w/v SIBS solution in oDCB.

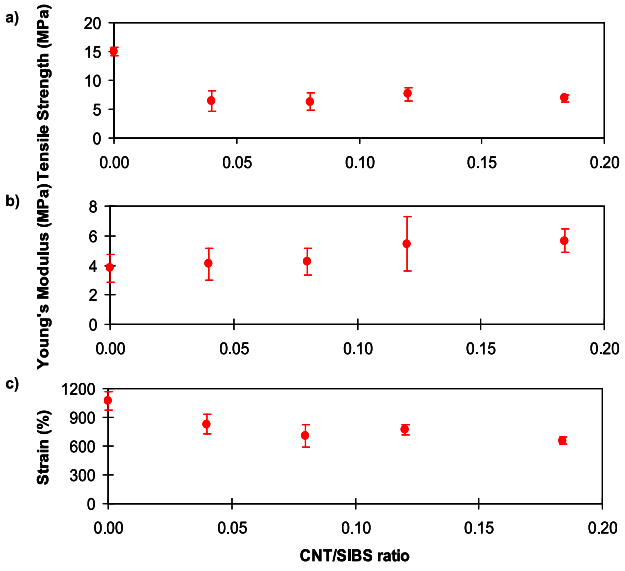

Figure 3. Dynamic mechanical analysis results for fibers made of SIBS and ODA-SWNT at different CNT/SIBS ratios: 0.00, 0.04, 0.08, 1.20, 1.84 CONT/SIBS ratio; (a) tensile strength, (b) Young's modulus and (c) strain.

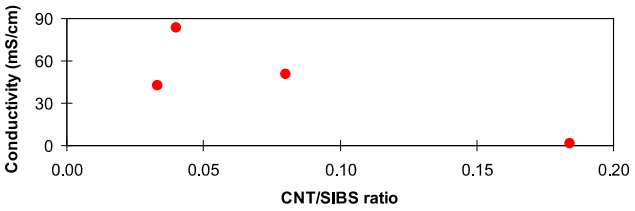

Figure 4. The electrical conductivity of fibers as a function of ODA-SWNT/SIBS ratios: 0.03, 0.04, 0.08, 1.8 CONT/SIBS ratio.

Increasing the ODA-SWNT content above 0.4% w/v rapidly decreased conductivity values, as shown in Fig. 4.

D. *Strain Gauging*

Strain gauging was carried out on an ODA-SWNT/SIBS fiber (conductivity 84 mS/cm) with the conductivity normalized to the initial (pre-strained) value, i.e. σ/σ_0. During strain gauging the conductivity displays two maxima (Fig. 5). The conductivity increases with increasing strain between 10% and 23%, before a rapid decrease between 23% and 30% strain. On the reversing strain cycle (from 30% strain to 10%), conductivity increases with decreasing strain (30% to 23%), then it decreases between 23% and 10% strain.

The ODA-SWNT forms a so-called pseudo-percolative network in the fiber, which under strain results in an increase in number of connecting paths [7]. However, further straining eventually leads to a decrease in number of conducting paths

The conductivity of a true percolative network of ODA-SWNT would increase with increasing strain. The different behaviour for our fiber is likely to be a result of the ODA-SWNT forming clusters or aggregates within the fiber. At low strain levels the reduction in diameter increases the number of conducting paths but further straining results in disrupting the connections between the clusters. The latter results in a decreasing number of conducting pathways, i.e. decreased conductivity (Fig. 6). The observation that the conductivity values recovered after the strain was relaxed supports this suggestion.

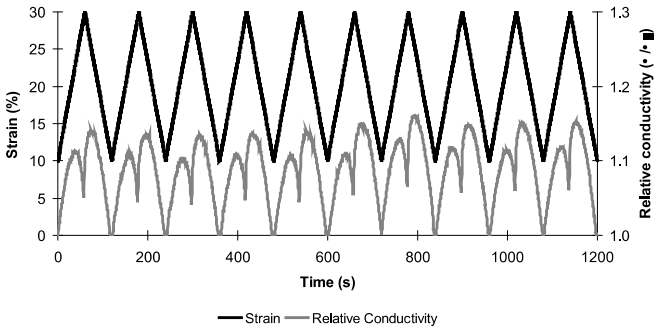

Figure 5. Evolution of the relative conductivity (conductivity at any given point divided by the initial conductivity, σ_0 = 84 mS/cm) of a piece of fiber under constant potential, DC 10V, during strain-gauge cycles.

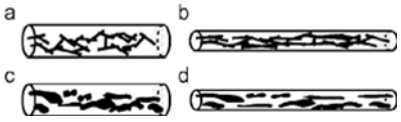

Figure 6. Schematic representation of (a) CNT percolative network relaxed state, (b) CNT percolative network under strain; (c) CNT cluster network relaxed state and (d) CNT cluster network under strain.

Similar responses have been observed for carbon black filled silicone rubber [16, 17]. The authors attributed this to conducting filler forming discrete structures within the elastomeric polymer matrix, which initially results in close contact at low strains, but these separate from each other under increased strain. This results in a reduction in the conductivity of the sample, as observed in Fig. 5.

IV. CONCLUSIONS

We report the fabrication of elastic conducting fibers using a continuous flow wet-spinning approach. Strain, tensile strength and Young's modulus values of 828%, 6.9 MPa and 5.7 MPa, respectively were easily achieved. The tensile strength and ductility values decreased with the addition of ODA-SWNT, which was attributed to the formation of nanotubes aggregates within the fiber rather than a homogeneous network of nanotubes. The results from strain gauging experiments support this suggestion. The initial conductivity of fibers (84 mS/cm) increased under strain until separation of cluster lead to a decrease in conductivity. This process was reversible and repeatable over several cycles.

ACKNOWLEDGEMENTS

This work was supported by the University of Wollongong, Boston Scientific Corporation and the Australian Research Council (ARC), ARC Federation Fellowship (G.G. Wallace) and ARC Future Fellowship (M. in het Panhuis).

REFERENCES

[1] L. Pinchuk, G.J. Wilson, J.J. Barry, R.T. Schoephoerster, J.-M. Parel, J.P. Kennedy, Biomaterials, 29, 448-460 (2008).

[2] S.V. Ranade, R.E. Richard, M.N. Helmus, Acta Biomaterialia, 1, 137-144 (2005).

[3] A.C. Acosta, E.M. Espana, H. Yamamoto, S. Davis, L. Pinchuk, B.A. Weber. *et al*., Archives of Ophthalmology, 124, 1742-1749 (2006).

[4] W. Yin, S. Gallocher, L. Pichuk, R. Schoephoerster, J. Jesty, D. Bluestein, Atificial Organs, 29, 826-831 (2000).

[5] S. Rosset, M. Niklaus, P. Dubois, H.R. Shea; Adv. Funct. Mater., 19, 470-478 (2009).

[6] S. Pavlosky, A. Siegmann; J. Appl. Polym. Sci., 114, 1390-1396 (2009).

[7] T.S. Hansen, K. West, O. Hassager, N.B. Larsen; Adv. Funct. Mater., 17, 3039-3073 (2007).

[8] A. Das, K.W. Stöckelhuber, R. Jurk, M. Saphiannikova, J. Fritzsche, H. Lorenz, M. Klüppel, G. Heinrich; Polymer, 49, 5276-5283 (2008).

[9] K.J. Gilmore, S.E. Moulton, G.G. Wallace, Carbon, 45, 402-410 (2007).

[10] Y. Liu, K.J. Gilmore, J. Chen, V. Misoska, G.G. Wallace; Chem. Mater., 19, 2721-2723 (2007).

[11] A.F. Quigley, J.M. Razal, B.C. Thompson, S.E. Moulton, M. Kita, E.L. Kennedy, *et al*., Advanced Materials, 21, 4393-4397 (2009).

[12] E.H. Immergut, E.A. Grulke, Polymer Handbook, Eds. J. Brandrup, 4th ed., New York: John Wiley, 1999, pp.675-711.

[13] M. Belmares, M. Blanco, W.A. Goddard III, R.B. Ross, G. Caldwell, S.-H. Chou, J. Pham, P.M. Olofson, C. Thomas, Journal of Computational Chemistry, 25, 1814-1826 (2004).

[14] J.L. Bahr, E.T. Mickelson, M.J. Bronikowski, R.E. Smalley, J.M. Tour, Chemical Communications, 193-194 (2001).

[15] J. Amiran, V.Nicolosi, S.D. Bergin, U. Khan, P.E. Lyons, J.N. Coleman, Journal of Physical Chemistry C, 112, 3519-3524 (2008).

[16] J. Kost, M. Narkis, A. Foux; Polym. Eng. Sci., 23, 567-571 (1983).

[17] J. Kost, M. Narkis, A. Foux; J. Appl. Polym. Sci., 29, 3937-3946 (1984).